

Finite Length Horizontal Dipole over a Ground Plane

Simulated Beam vs Analytical Beam Study

Part 1

Tom Mozdzen

11/11/2014

Summary

A comparison of the convolved response of a dipole antenna with the sky was made between two finite length dipoles over a ground plane. The first beam is a simulated beam derived from CST results and the second beam is an analytical beam. The comparison metric was the RMS Error of a polynomial fit in $\log^n(\nu)$ of the antenna's response to a frequency scaled (index 2.5) Haslam Skymap. The frequency range used was 100 to 190 MHz. The number of terms of interest ranged from $n=3$ to $n=5$.

In this study, the varied parameters were the amount of simulation space added to the CST simulations, the wire diameter of the dipole, and the gap distance between the two segments. It was found that extra space added to the simulations resulted in additional structure to the CST beam which increased the RMS error for a given polynomial order. An issue with the CST simulated beam was observed in the low frequency range between 100 and 120 MHz in that the beam failed to vary smoothly. The analytical dipole's RMS error was found to be lower than the CST derived model and had no smoothness issue in any part of the frequency range. A follow up study will need to be performed to investigate better ways to set CST accuracy limits via simulation variables and meshing schemes.

Method

The analytical beam was computed using a classic infinitely thin $\frac{1}{2} \lambda$ dipole, $\frac{1}{4} \lambda$ over a ground plane and is expressed by

$$Beam = \left[\frac{(\cos(kL/2 \cdot \cos \theta') - \cos(kL/2))}{\sin \theta'} \right]^2 \left[\sin^2 \left(\frac{\pi h}{2} \cos \theta \right) \right],$$

where L is the total length of the dipole, h is the height of the dipole above the ground plane in units of wavelength fraction given by

$$h = \left(\frac{\nu}{\nu_{height}} \right) = \left(\frac{\lambda_{height}}{\lambda} \right), \text{ and}$$

$$\theta' = \cos^{-1}(\sin \theta \sin \phi),$$

where, θ and ϕ are spherical coordinates, and $\nu_{height} = 176.7$ MHz. The excitation axis is aligned with $\phi = 0^\circ$.

The three parameters varied were the space between the physical structure and the simulation bounding box expressed in fractions of a wavelength, the diameter of the wire, and the gap between the two wires. The wire was placed above an infinite ground plane at a distance equal to $\frac{1}{4} \lambda$ at 176.7 MHz, chosen to mimic the beam structure near the zenith of the EDGES antenna. Tables 1 and 2 below list the parameters of the 19 simulation variations.

The data presented in the results section are 1) the 3 dB half beam width values of the beam measured for the simulations and compared against the theoretical calculations; 2) Beam patterns sliced at $\phi=0^\circ$ (the excitation axis) and $\phi=90^\circ$ at several frequencies; 3) Plots of the RMS error for a fixed latitude of -26° vs LST for the various beams; and 4) Beam derivatives wrt frequency vs frequency coupled with a slice through a fixed theta to reveal beam smoothness.

Results

Beam Shape

We begin by comparing the normalized 3 dB half beam width values of the simulated beams to the analytical beams. We can see in Figs. 1a and 1b that the values match better for $\phi=90^\circ$ ($<0.2^\circ$) than for $\phi=0^\circ$, and are fairly steady as the run parameters are varied. Differences might be attributed to the fact that there is a gap in the simulation and that the wires have a finite diameter.

Figures 2a-4b illustrate that the beam patterns qualitatively match the analytical expression, and that the differences which produce different RMS errors must be subtle, as the curves are indistinguishable at this scale.

RMS Error vs LST

Figure 5a shows the RMS error vs run number for an LST region which yields low RMS error values and Figure 5b shows an LST region which yields high RMS error values, at -26° latitude. One can see that the RMS error generally decreases as the amount of extra simulation space is decreased.

The RMS Error vs LST plot using the theoretical beam is shown in Figure 6a and for the CST derived beam of Run 19 is shown in Figure 6b. The residuals at an LST value of 4.0 hrs are plotted vs frequency in Figure 7a for the analytical beam and in 7b for the simulated beam. The fit of low order polynomials are very similar in the two cases, but there is more structure in the CST derived beam as the residual errors are not removed when the order of the polynomial is increased as they are in the theoretical beam.

Runs 1-10 shown in Figures 8-12, show the RMS Error vs LST for various cases of extra simulation space ranging from 1 full wavelength through $1/16$ wavelengths, where each case has two subcases where the wire diameter is varied from 0.05" to 0.10" while the gap is kept constant at 0.50". The thinner wire generally helped the RMS error, but the extra space was still the overriding factor.

Runs 11-21 focused on varying the dipole wire diameter and the gap spacing and were run using the least amount of simulation space ($\lambda/32$) as this usually gave the best results. Runs 16 and 19 used wire diameters of 0.05" and a gap of 0.05" and 0.50" respectively and yielded the lowest RMS error values

at LST = 4.0 hrs. However, the errors were still much higher than the analytical results, so further investigation was pursued.

Beam Derivatives

The smoothness of the beam was evaluated by taking the derivative of the beam wrt frequency. That is, for each beam value at a given θ and φ , the difference between the value at one frequency and the next frequency (1 MHz away) was taken and in this manner a derivative pcolor plot was made. Figures 14a-15b display the pcolor plots for CST runs 19 and 7. Irregularities can be seen in the lower frequencies. A cut line through the value of $\theta=40^\circ$ was plotted and is shown in Figures 16a-17b. It is clear that CST is having trouble accurately calculating the beam for the lower frequencies. Figures 18-21 show the same data for the analytical beam. These lines are very smooth and in general, agree with the CST results except for the lower frequencies. The conclusion is that a second study is needed to figure out how to get CST to yield better dipole beam patterns.

Short Dipole

On a side note, the jaggedness of the cut lines through $\theta=40^\circ$ is not causing issues with the fit. CST does a very good job handling a short dipole over a ground plane. The residuals are less than 0.1 mK even with the presence of these ripples.

One possible source of the jaggedness was postulating that it might be due to the fact that the CST beam data output only contains 4 significant figures. The only way to get more digits is to output the electric field. This was checked for one beam pattern, but the output still contained the jagged edges.

Conclusions

With the given meshing scheme and accuracy settings presented, CST can simulate the finite dipole over a ground plane accurately to a certain degree. But, for EOR detection, higher accuracy is needed. Differences of 0.001 are enough to cause 100s of mK of extra RMS error when fitting a polynomial to the antenna response.

CST is adding more structure to the beam by inaccurately calculating the beam at low frequencies. Adding extra space to the simulation only makes the problem worse. The gap and diameter of the wire is important, but it is not the cause of the low frequency inaccuracy. The next step is to perform a meshing and accuracy study, that is, a Part 2 is needed.

Parameter	Value
Mesh Type	PBA
Lines per Wavelength	75
Lower Mesh Limit	45
Mesh Ratio Limit	65
Solver Accuracy	-50 dB
Edge Enhancement	85%
Frequency Range of Simulation	80 to 220 MHz
Frequency to Calculate Extra Space	100 MHz
Reflection at Boundaries	1×10^{-4}

Table 1. Common Simulation Parameters

Simulation Number	Simulation Boundary Distance to Structure (λ fraction @ 100 MHz)	Wire Diameter (inches)	Center Gap (inches)
1	1	0.05	0.50
2	1	0.10	0.50
3	1/2	0.05	0.50
4	1/2	0.10	0.50
5	1/4	0.05	0.50
6	1/4	0.10	0.50
7	1/8	0.05	0.50
8	1/8	0.10	0.50
9	1/16	0.05	0.50
10	1/16	0.10	0.50
11	1/32	0.010	0.010
12	1/32	0.010	0.50
13	1/32	0.025	0.025
14	1/32	0.025	0.500
15	1/32	0.050	0.025
16	1/32	0.050	0.050
17	1/32	0.050	0.100
18	1/32	0.050	0.250
19	1/32	0.050	0.500
20	1/32	0.050	0.750
21	1/32	0.10	0.50

Table 2. Description of the parameter settings for the CST runs.

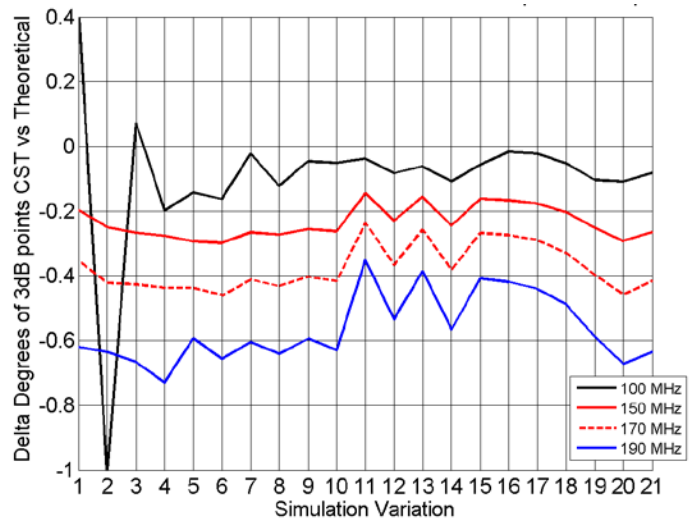
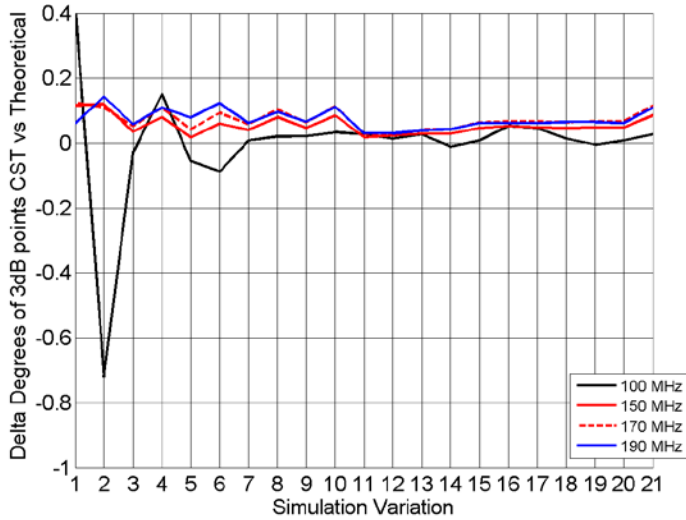


Figure 1a. Difference between CST obtained 3dB beam width and analytical values vs Run. At $\Phi=90^\circ$.

Figure 1b. Difference between CST obtained 3dB beam width and analytical values vs Run. At $\Phi=0^\circ$.

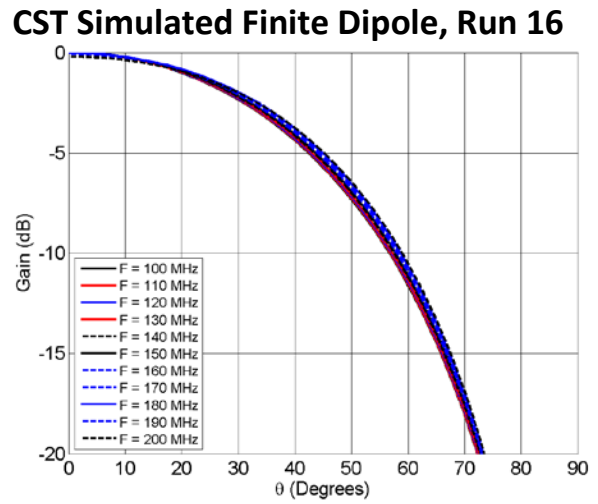
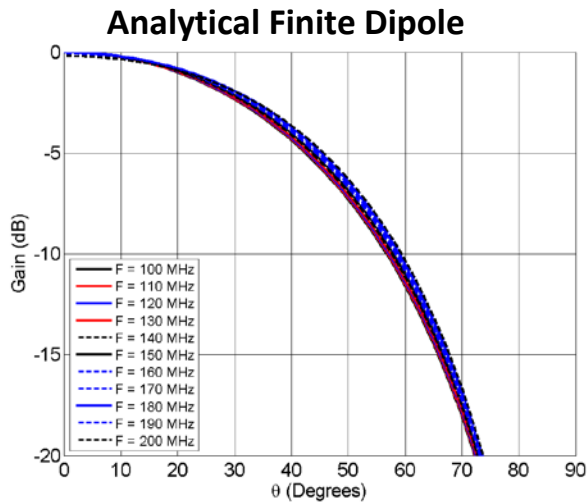


Figure 2a. Beam vs Theta at $\phi=0^\circ$.

Figure 2b. Beam vs Theta at $\phi=0^\circ$.

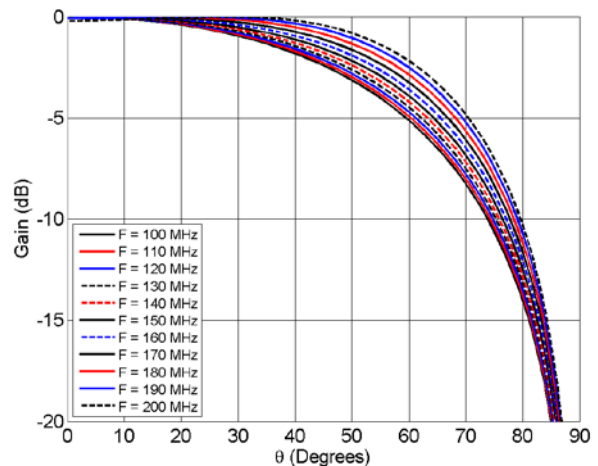
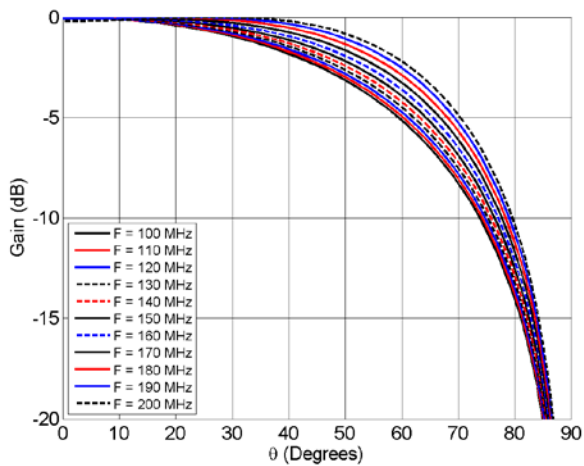


Figure 3a. Beam vs Theta at $\phi=90^\circ$.

Figure 3b. Beam vs Theta at $\phi=90^\circ$.

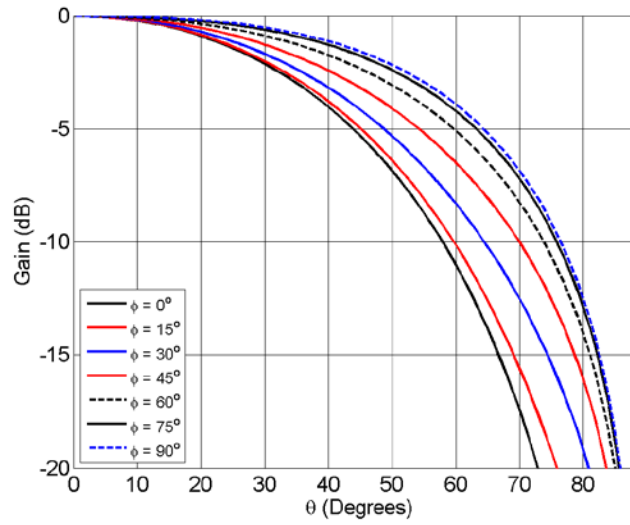


Figure 4a. Beam vs Theta at 150 MHz.

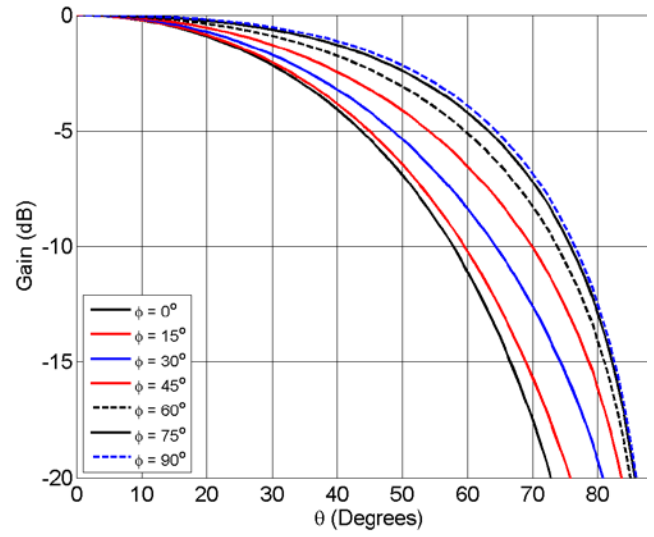


Figure 4b. Beam vs Theta at 150 MHz.

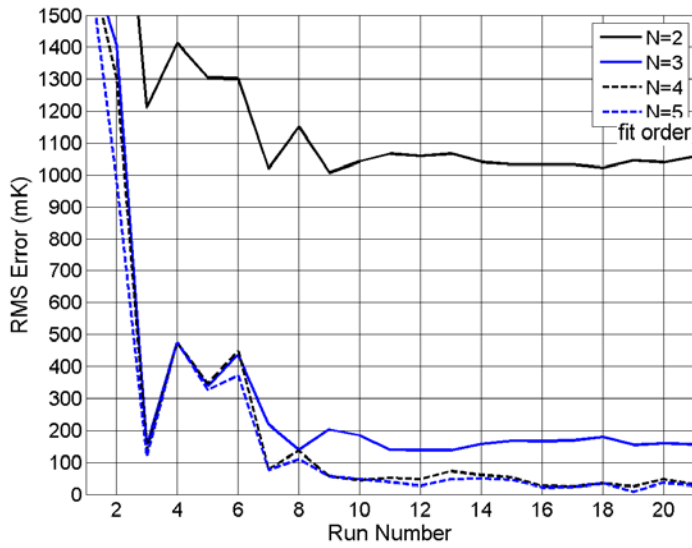


Figure 5a. High RMS error region, LST=17.3 hrs.

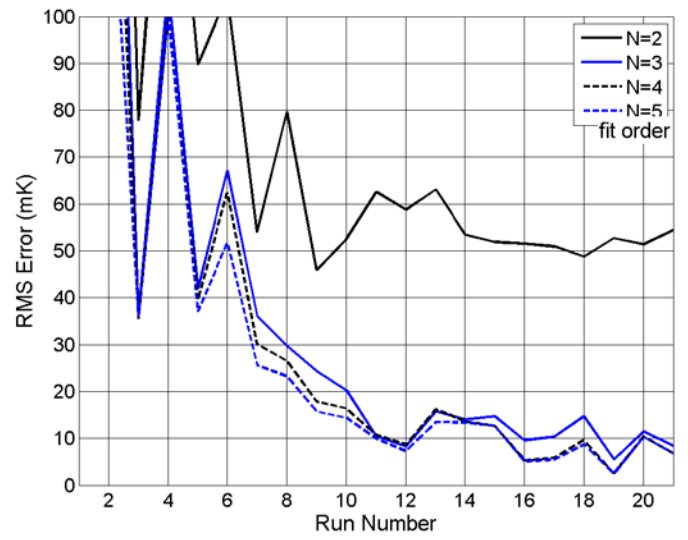


Figure 5b. Low RMS error region, LST = 4.0 hrs.

Analytical Dipole, Lat = -26, 100-190 MHz fit.

**CST Dipole, Lat = -26, 100-190 MHz fit.
Run 19: Added simulation space = $\lambda/32$,
wire diameter = 0.05", gap = 0.50".**

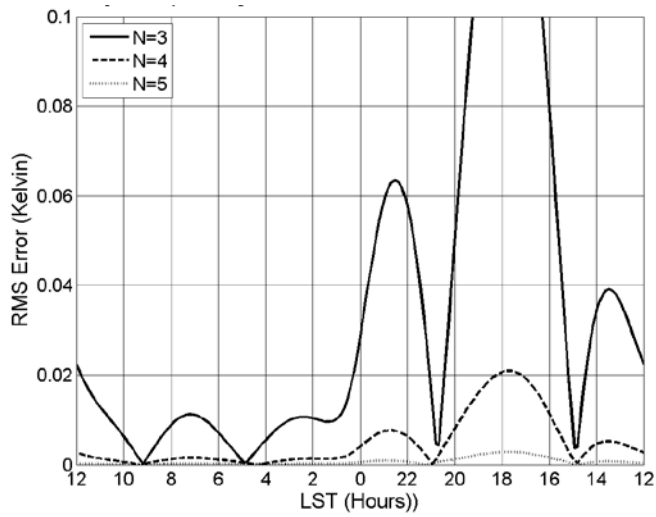


Figure 6a. RMS Error vs LST.

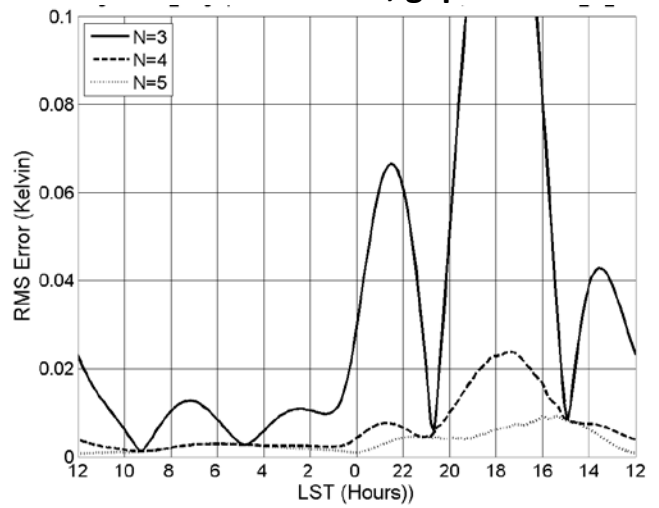


Figure 6b. RMS Error vs LST.

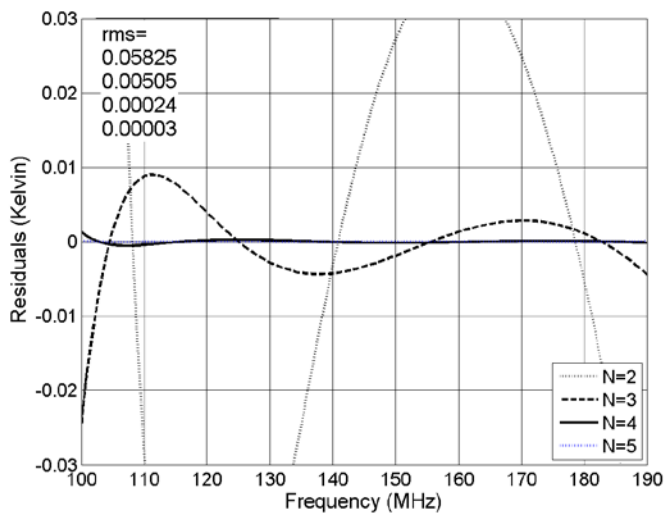


Figure 7a. Residuals vs frequency, LST = 4.0 hrs.

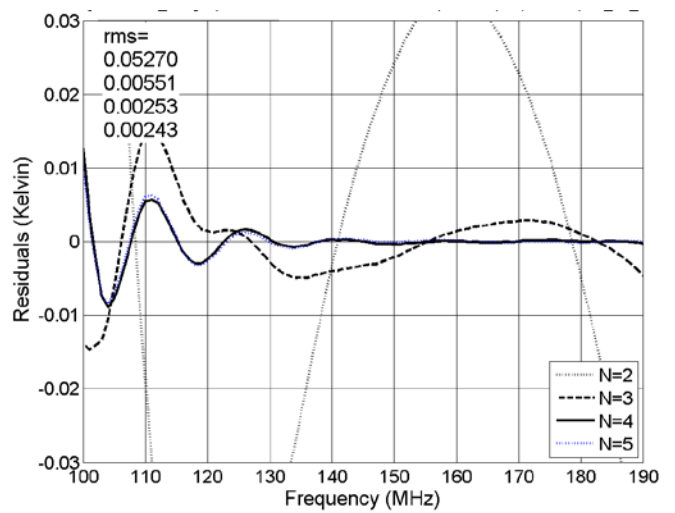


Figure 7b. Residuals vs frequency, LST = 4.0 hrs.

CST Dipole, Lat = -26, 100-190 MHz fit.
Wire diameter = 0.05", gap = 0.50".

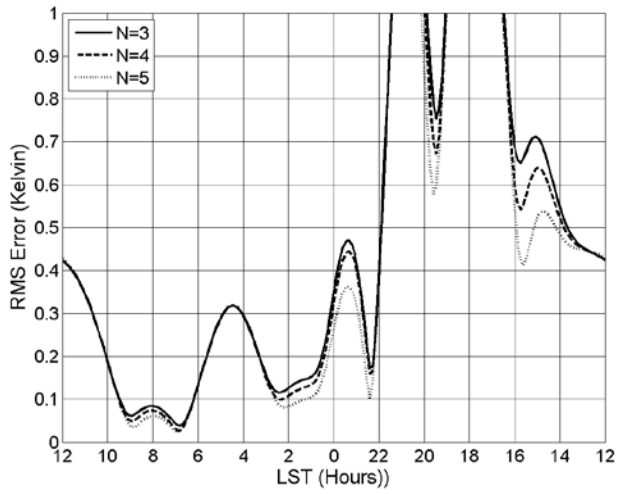


Figure 8a. Run 1. Extra Space Using $\lambda/1$.

CST Dipole, Lat = -26, 100-190 MHz fit.
Wire diameter = 0.10", gap = 0.50".

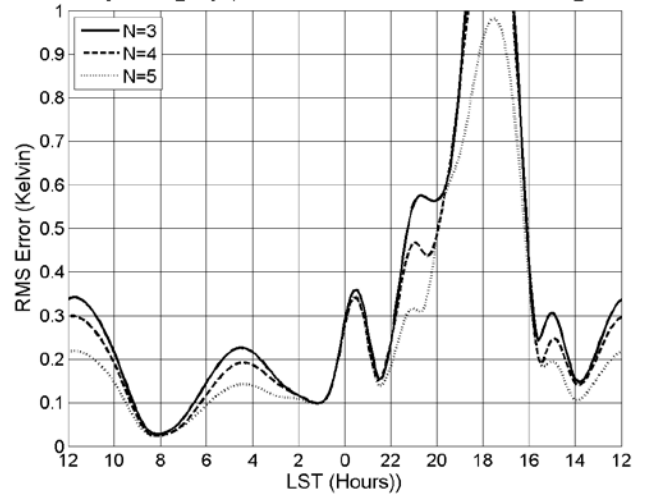


Figure 8b. Run 2. Extra Space Using $\lambda/1$.

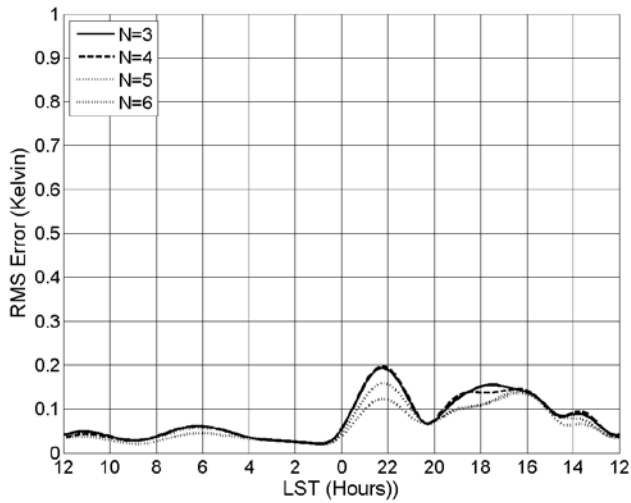


Figure 9a. Run 3. Extra Space Using $\lambda/2$.

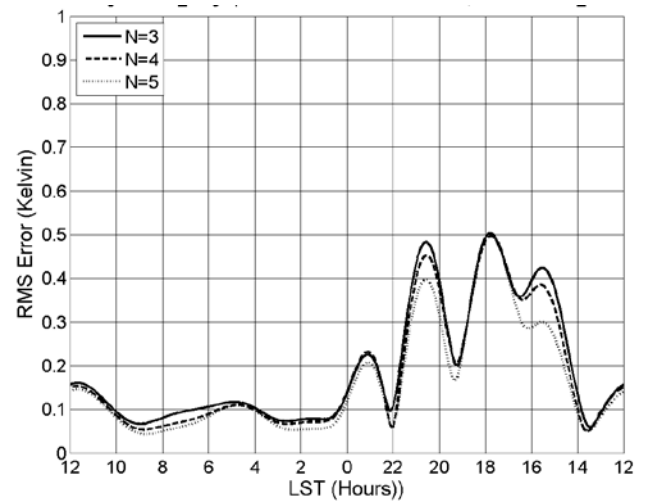


Figure 9b. Run 4. Extra Space Using $\lambda/2$.

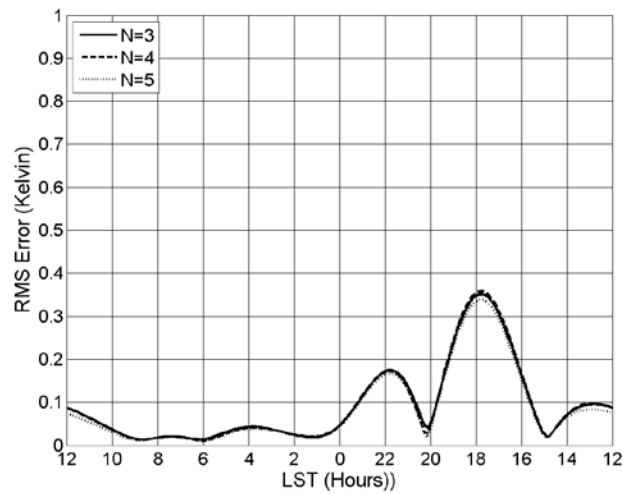


Figure 10a. Run 5. Extra Space Using $\lambda/4$.

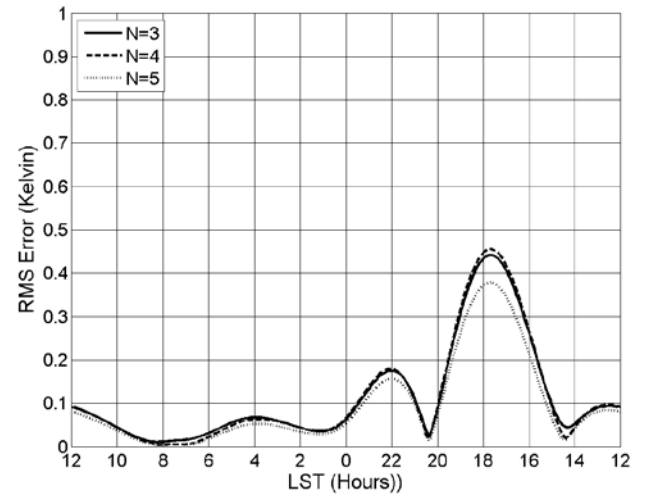


Figure 10b. Run 6. Extra Space Using $\lambda/4$.

CST Dipole, Lat = -26, 100-190 MHz fit.
Wire diameter = 0.05", gap = 0.50".

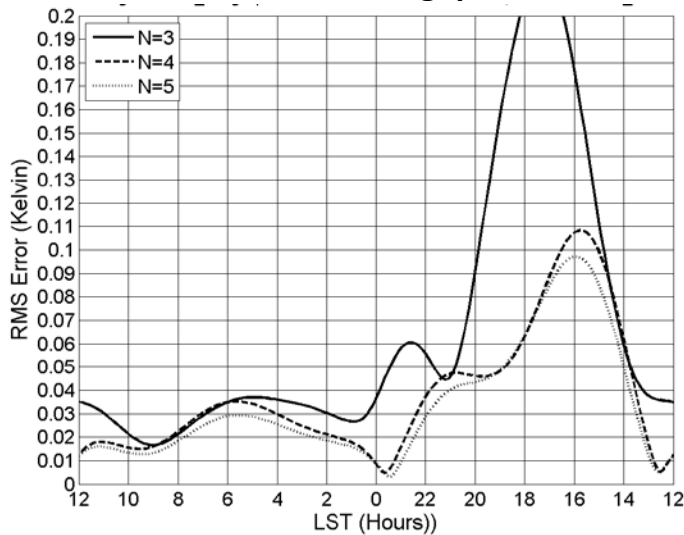


Figure 11a. Run 7. Extra Space Using $\lambda/8$.

CST Dipole, Lat = -26, 100-190 MHz fit.
Wire diameter = 0.10", gap = 0.50".

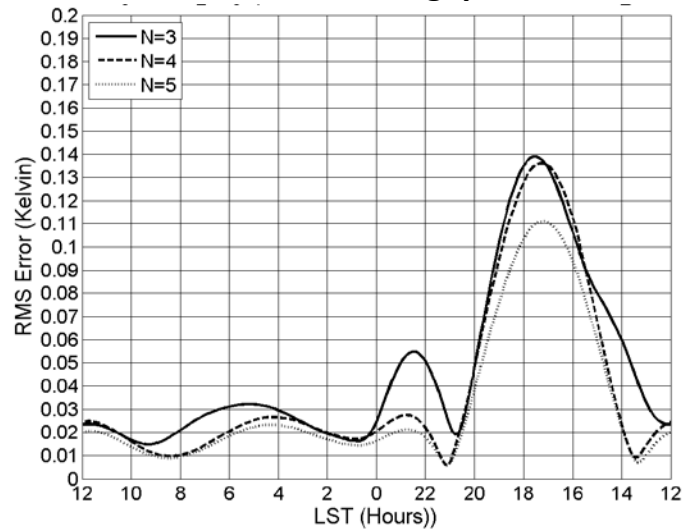


Figure 11b. Run 8. Extra Space Using $\lambda/8$.

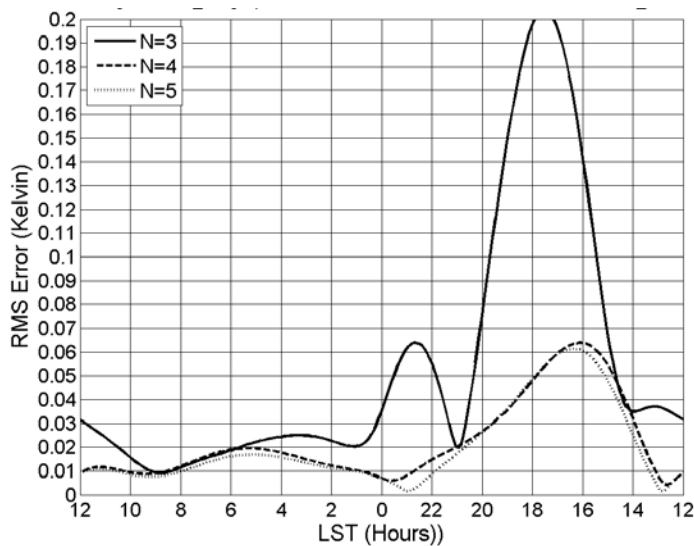


Figure 12a. Run 9. Extra Space Using $\lambda/16$.

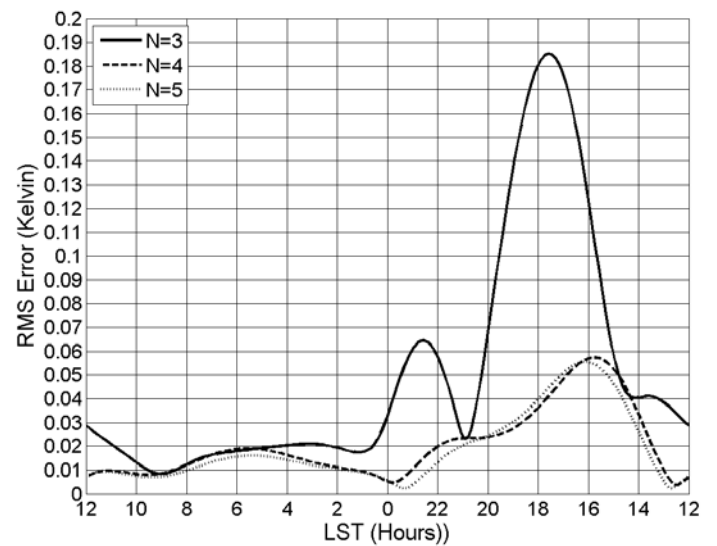


Figure 12b. Run 10. Extra Space Using $\lambda/16$.

CST Dipole, Lat = -26, 100-190 MHz fit.

Extra Space Using $\lambda/32$

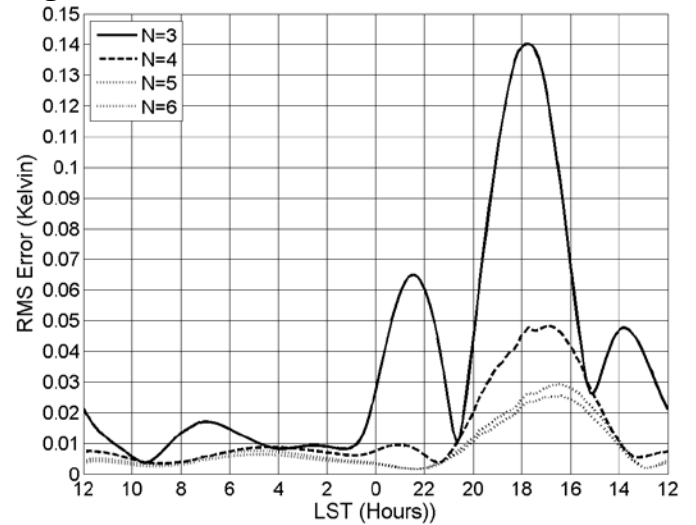
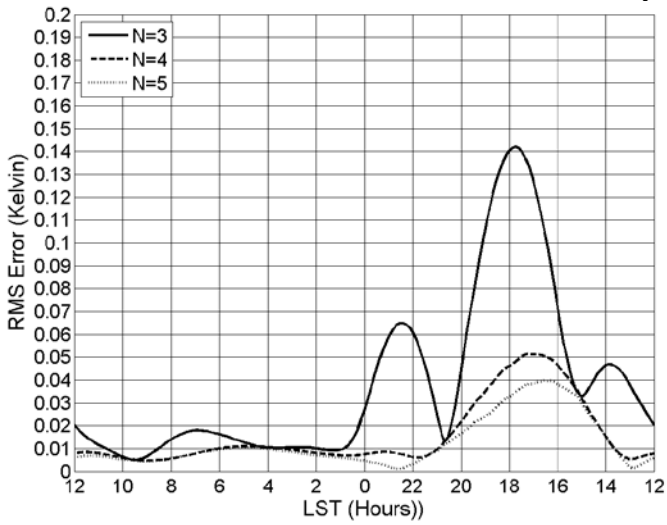


Figure 13a. Run 11. Wire diameter = 0.01", gap = 0.01".

Figure 13b. Run 12. Wire diameter=0.01", gap=0.50".

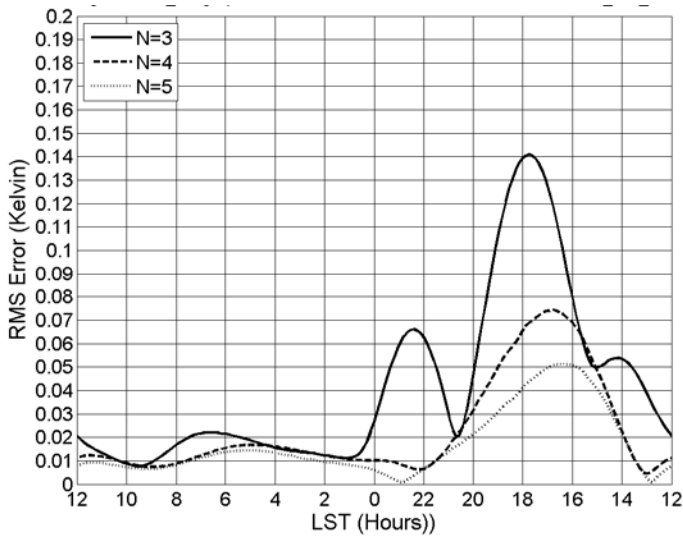


Figure 13c. Run 13. Wire diameter=0.025", gap=0.025".

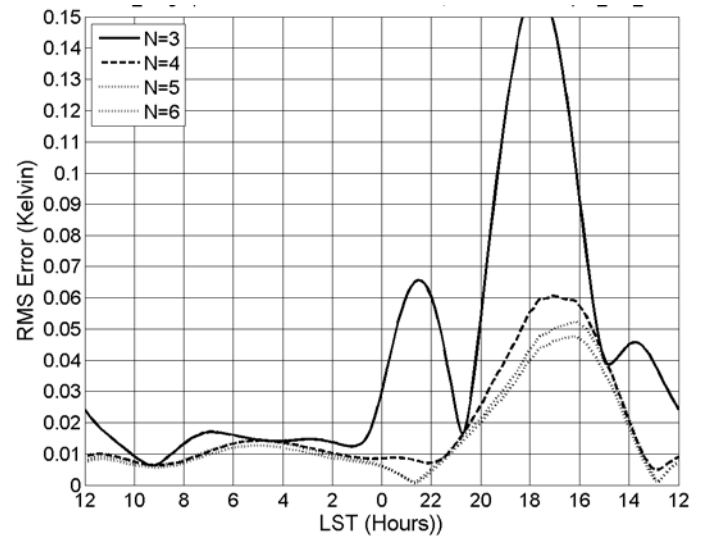


Figure 13d. Run 14. Wire diameter=0.025", gap=0.50".

CST Dipole, Lat = -26, 100-190 MHz fit.

Extra Space Using $\lambda/32$

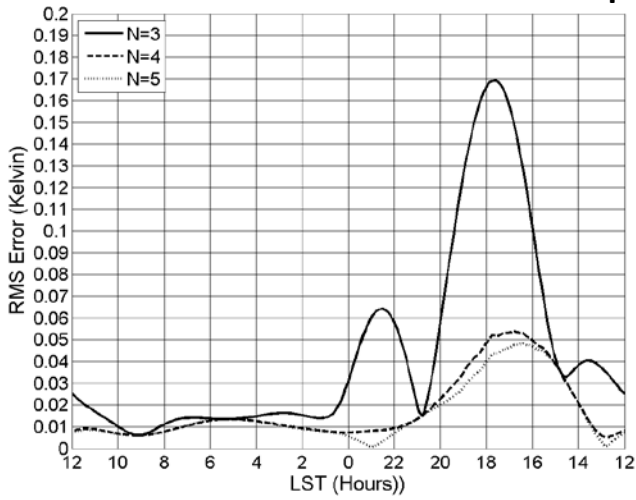


Figure 13e. Run 15. Wire diameter=0.05", gap=0.025".

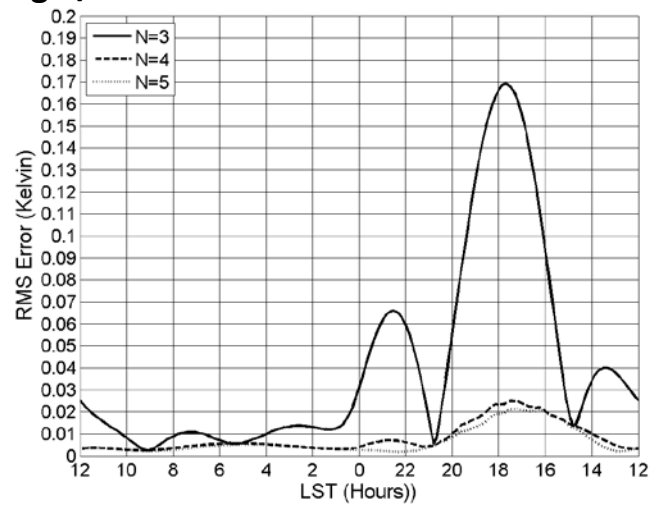


Figure 13f. Run 16. Wire diameter = 0.05", gap=0.05".

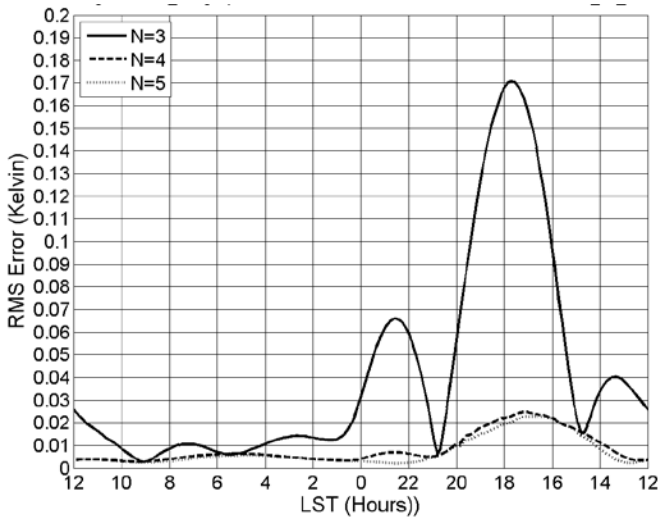


Figure 13g. Run 17. Wire diameter = 0.05", gap=0.10".

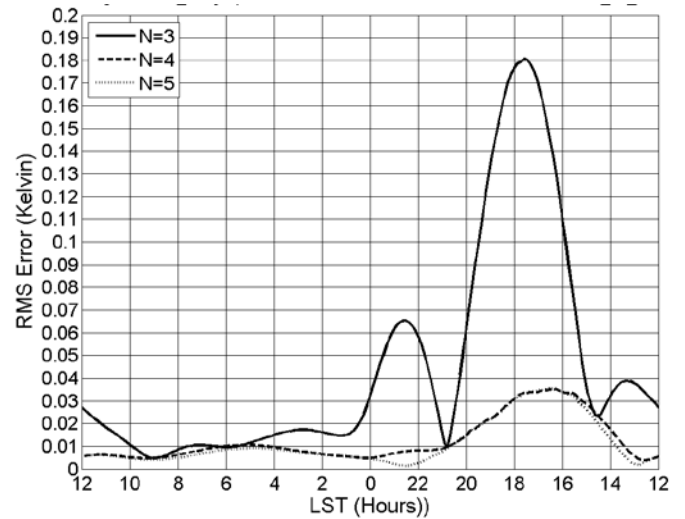


Figure 13h. Run 18. Wire diameter = 0.5", gap = 0.25".

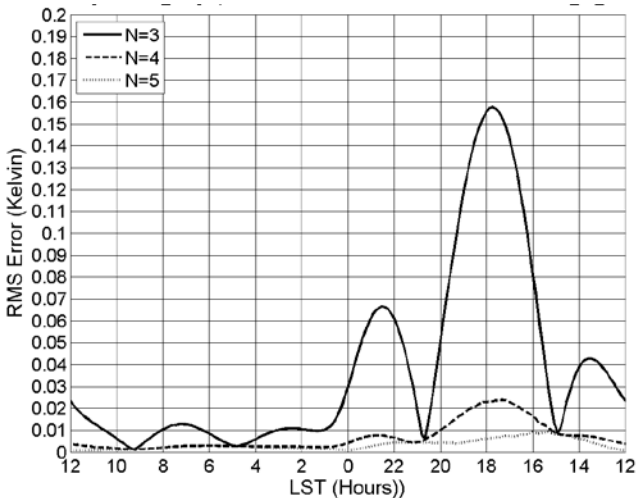


Figure 13i. Run 19. Wire diameter = 0.05", gap = 0.50".

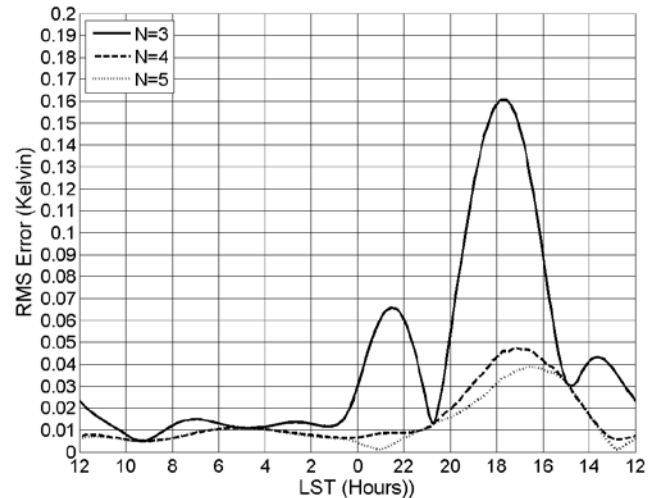


Figure 13j. Run 20. Wire diameter = 0.05", gap = 0.75".

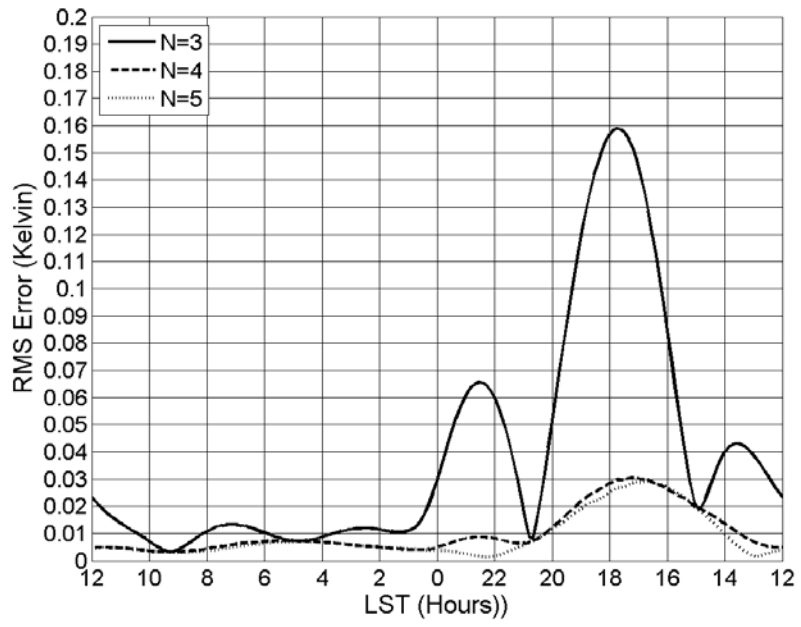


Figure 13k. Run 21. Wire diameter = 0.10", gap = 0.50".

CST Beam Run 19

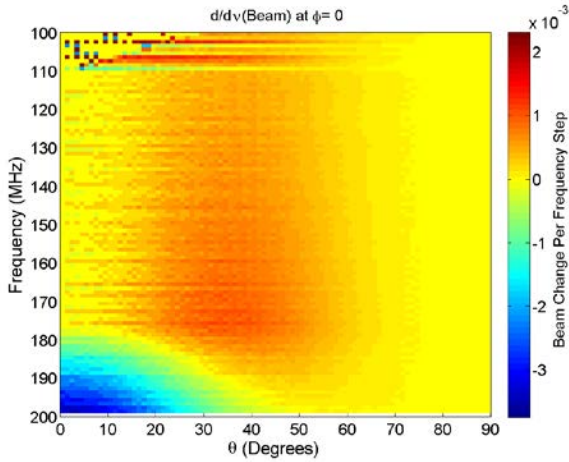


Figure 14a. Derivative plot for $\phi=0^\circ$.

CST Beam, Run 7

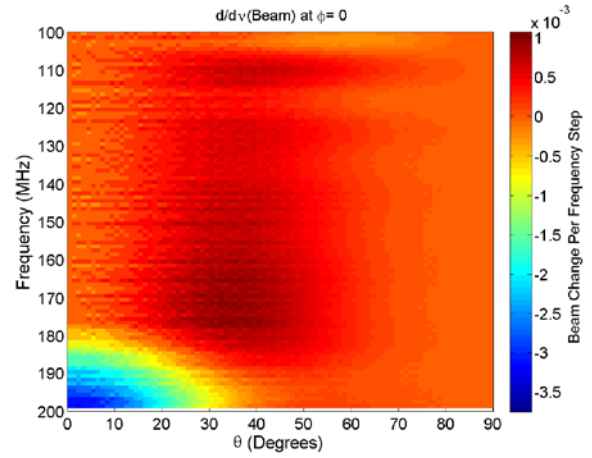


Figure 14b. Derivative plot for $\phi=0^\circ$.

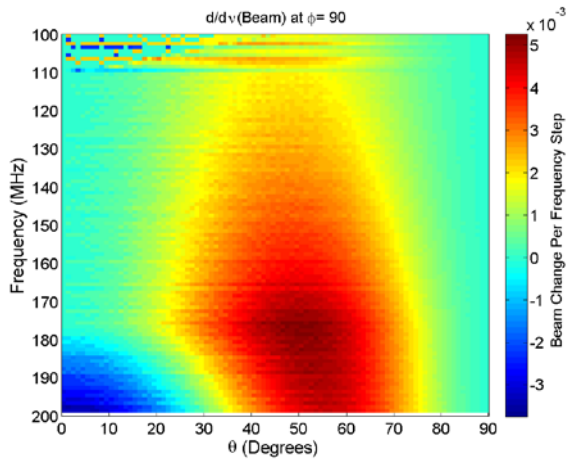


Figure 15a. Derivative plot for $\phi=90^\circ$.

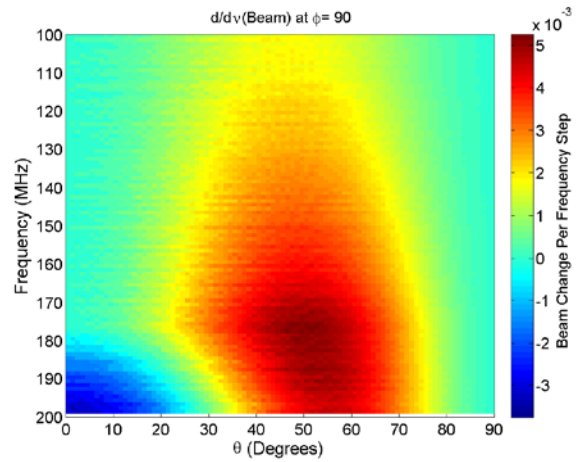


Figure 15b. Derivative plot for $\phi=90^\circ$.

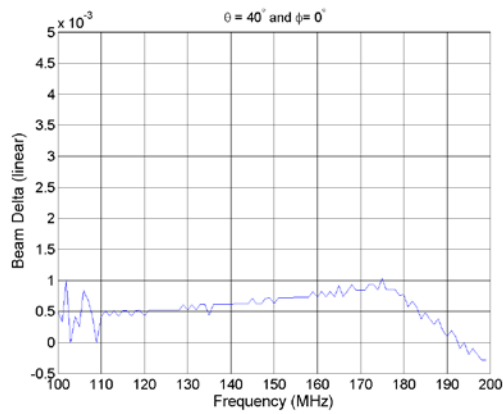


Figure 16a. $\phi=0^\circ$, $\theta=40^\circ$ cut line.

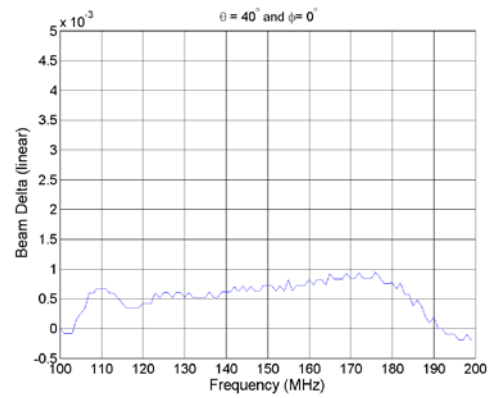


Figure 16b. $\phi=0^\circ$, $\theta=40^\circ$ cutline.

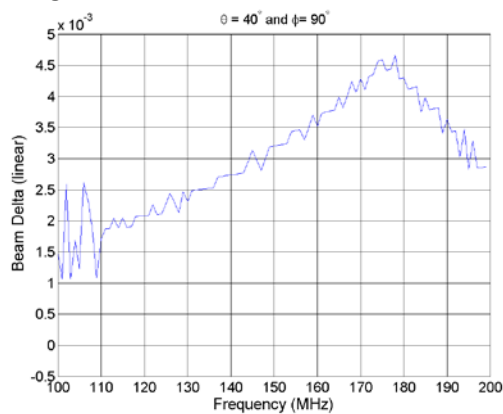


Figure 17a. $\phi=90^\circ$, $\theta=40^\circ$ cut line.

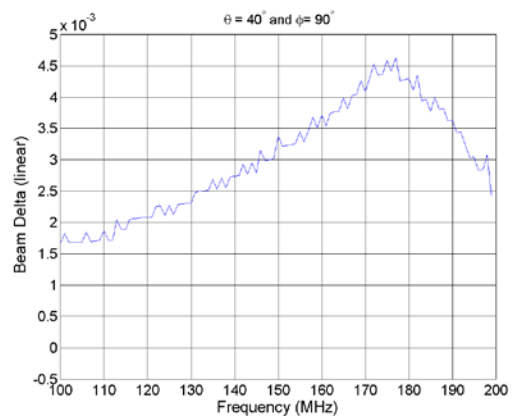


Figure 17b. $\phi=90^\circ$, $\theta=40^\circ$ cut line.

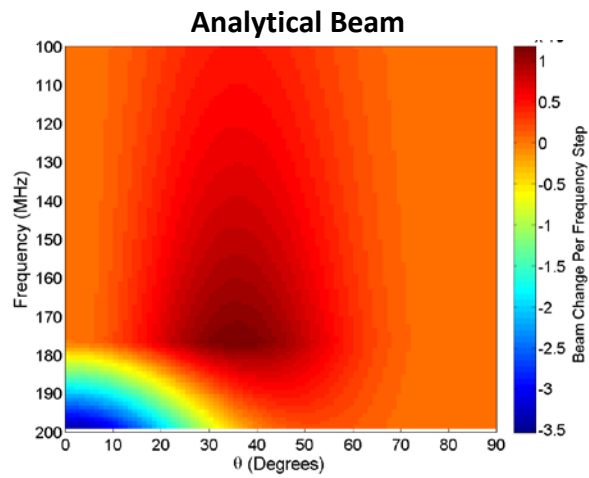


Figure 18. Derivative plot for $\phi=0^\circ$.

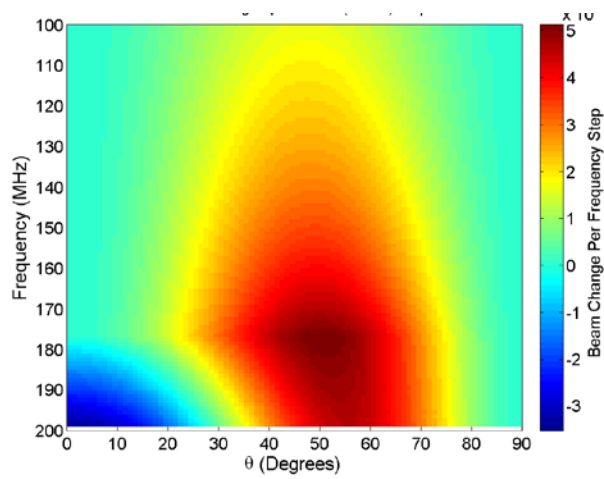


Figure 19. Derivative plot for $\phi=90^\circ$.

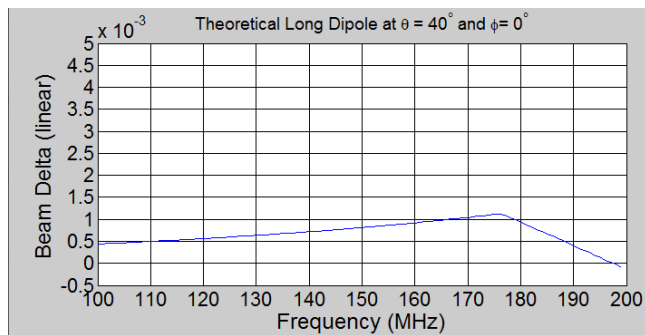


Figure 20. Cut through $\theta = 40^\circ$, $\phi=0^\circ$.

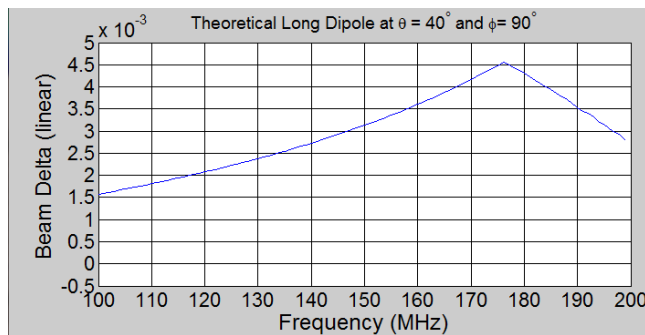


Figure 21. Cut through $\theta = 40^\circ$, $\phi=90^\circ$.